Kinetics of polyelectrolyte adsorption

1997 J. Phys.: Condens. Matter 9 7767

(http://iopscience.iop.org/0953-8984/9/37/009)

J. Phys.: Condens. Matter **9** (1997) 7767–7783. Printed in the UK PII: S0953-8984(97)80583-8

Kinetics of polyelectrolyte adsorption

M A Cohen Stuart, C W Hoogendam and A de Keizer

Department of Physical and Colloid Chemistry, Wageningen Agricultural University, PO Box 8038, 6700 EK Wageningen, The Netherlands

Received 2 January 1997, in final form 9 June 1997

Abstract. The kinetics of polyelectrolyte adsorption has been investigated theoretically. In analogy with Kramers' rate theory for chemical reactions we present a model which is based on the assumption that a polyelectrolyte encounters a barrier in its motion towards an adsorbing surface. The height of the barrier, which is of electrostatic origin, is calculated with a self-consistent-field (SCF) model. The salt concentration strongly affects the height of the barrier. At moderate salt concentrations ($\sim$0.2 mol l^{-1}) equilibrium in the adsorption is attained; at low salt concentration ($\sim$0.01 mol l^{-1}) equilibrium is not reached on the time scale of experiments. The attachment process shows resemblances to the classical DLVO theory.

1. Introduction

In the context of polymer adsorption, the question of reversibility is posed time and again. In the past, many experimental results have been taken as evidence for the existence of non-equilibrium states, and various explanations have been forwarded [1, 2]. Some observations could be explained without taking irreversibility into account, e.g., sample polydispersity effects ([3], ch 5 of [4]). However, it is obvious that kinetic barriers cannot be ignored, and that slow processes should be expected. Recent experimental work has therefore focused on kinetic aspects of adsorption and desorption, and various interesting slow surface processes were identified [5–8]. Also, quite general arguments were forwarded that can explain the apparent absence of desorption by solvent rinsing [9]. From the theoretical point of view, the problem of adsorption kinetics was recently studied in detail by Semenov and Joanny [10]. These authors made estimates of the rate of adsorption of a neutral polymer. An important aspect of their theory is a calculation of the barrier experienced by an incoming chain for which they apply a variant of Kramers' theory for reaction rates [11].

It is somewhat surprising, however, that adsorption kinetics of polyelectrolytes has not yet been considered theoretically. Polyelectrolytes experience not only short-range interactions between their segments and the adsorbent surface, but also rather strong electrostatic interactions. In particular, when short-range attraction competes with electrostatic repulsion, one may anticipate a situation in which a strong electrostatic barrier impedes adsorption that would be thermodynamically allowed. This situation is very akin to that of charged colloidal particles that remain stable despite the lower free energy of the aggregated state, simply because of an insurmountable kinetic barrier of electrostatic origin [12].

Strong hysteresis effects have indeed been observed in several experimental studies of polyelectrolyte adsorption. For example, polyelectrolytes with weakly dissociating groups can be adsorbed to substantially higher amounts if, instead of adsorbing at a fixed pH, one

0953-8984/97/377767+17$19.50

goes through a pH cycle, i.e., the polymer is first adsorbed at a pH where it has (very) little charge, after which the polymer is charged up by a shift in pH; this has been termed 'enhanced adsorption' [13]. Another observation pointing to the presence of a kinetic barrier is the interaction between two mica surfaces covered with (positively charged) polylysine, as measured by Luckham and Klein in the surface-force apparatus [14]. Upon first approach, these authors found a long-range repulsion, which disappeared once the two surfaces were brought close together. This strongly suggested the presence of long dangling ends that needed to be pushed through a barrier in order to adsorb. With neutral polymer, such behaviour has never been found.

Recently we have studied the adsorption of carboxymethyl cellulose (CMC) on inorganic oxide particles (TiO_2, α-Fe_2O_3) as a function of pH, ionic strength, and polymer structure (degree of carboxylate substitution, chain length). The results showed features similar to those discussed above. In particular, the effect of a pH cycle was very pronounced [15].

In connection with the above-mentioned features we wondered to what extent electrostatic repulsion played a role in the adsorption kinetics, and we decided to tackle this problem theoretically. Our paper is organized as follows. We first briefly review the basic rate equation which is solved using the approach introduced by Semenov and Joanny in combination with a self-consistent-field (SCF) theory for (polyelectrolyte) adsorption. Then the SCF method is described by which the height of the adsorption barrier as a function of coverage is obtained. In the results section we first discuss equilibrium adsorption of polyelectrolytes which have an additional non-Coulombic ('specific') interaction with the substrate. This is followed by a set of numerical results for the rate of adsorption under a variety of experimental conditions. In particular kinetic adsorption curves are calculated. These curves are used to determine the extent of reduction of the adsorbed amount due to kinetic factors assuming realistic experimental time scales. Finally, we discuss our kinetic model bearing in mind relevant experimental data.

2. Theory

A polymer molecule, moving to an adsorbent surface, meets a number of resistances. At large distance from the surface there is the resistance due to transport in solution, where the mechanisms of convection and diffusion operate. Next, there can be a barrier in the proximity of the surface, e.g., due to the presence of a layer of adsorbed polymer molecules, or due to an electrical field. We assume that this barrier operates over short distances as compared to the transport contribution. We now suppose that, shortly after starting an experiment, a stationary state is established, where the concentration profile in the solution changes only very slowly with time. One can then write for the mass transport of polymers towards the surface J_t

$$R_t J_t = c_b - c_s(\Gamma). \tag{1}$$

Here J_t is expressed in moles per square metre per second, c_b is the bulk concentration far from the interface, and c_s is the subsurface concentration (mol m^{-3}) at absorption, i.e., the concentration of free polymer molecules that find themselves just near the adsorption barrier. R_t is the transport resistance in seconds per metre, which depends on the hydrodynamic conditions and on the diffusion coefficient [16]. For example, in an impinging-jet geometry, R_t is given by [17]

$$R_t^{-1} = 0.776(V\overline{\alpha})^{1/3}(D/r)^{2/3} \tag{2}$$

where V is the fluid velocity, $\overline{\alpha}$ a dimensionless streaming intensity parameter, r the radius of the inlet tube and D the diffusion coefficient of the polymer. The molecules that have

reached the barrier can pass in both directions (adsorption and desorption). The forward flux of adsorbing molecules $(\mathrm{d}\Gamma/\mathrm{d}t)_{fw}$ must obey first-order kinetics with respect to the subsurface concentration:

$$R_b(\Gamma)\left(\frac{\mathrm{d}\Gamma}{\mathrm{d}t}\right)_{fw} = c_s(\Gamma) \tag{3}$$

where R_b is the barrier resistance including the effect of a partial coverage of the surface. In order to obtain the backward flux, we note that in equilibrium backward and forward flux must be balanced. Hence, the backward flux $(\mathrm{d}\Gamma/\mathrm{d}t)_{bw}$ (desorption of polymers) is given by

$$R_b(\Gamma)\left(\frac{\mathrm{d}\Gamma}{\mathrm{d}t}\right)_{bw} = -c_{eq}(\Gamma) \tag{4}$$

where c_{eq} is the equilibrium concentration corresponding to a particular value of Γ. The net flux $(\mathrm{d}\Gamma/\mathrm{d}t)$ is given by the sum of the forward and backward contributions. For not too short times, the flux reaches a steady state situation, and $J_t = \mathrm{d}\Gamma/\mathrm{d}t$ [7]. Obtaining the net flux from equations (3) and (4) after elimination of c_s we arrive at

$$\left[R_b(\Gamma) + R_t\right]\frac{\mathrm{d}\Gamma}{\mathrm{d}t} = c_b - c_{eq}(\Gamma) \tag{5}$$

where both R_b and c_{eq} are functions of Γ. The dependence is such that R_b increases with adsorption; c_{eq} and Γ are related by means of an adsorption isotherm. Equation (5) suffices to calculate the rate of the adsorption process, provided the equilibrium adsorption isotherm $\Gamma(c_{eq})$ and the barrier resistance $R_b(\Gamma)$ are known. Finally, integration leads to the time-dependent adsorption $\Gamma(t)$.

In order to obtain the barrier resistance, we use as do Semenov and Joanny [10], the Kramers equation:

$$R_b(\Gamma) = \int \frac{1}{D'}\,\mathrm{e}^{u(\Gamma,\,z^*)/kT}\,\mathrm{d}z^*. \tag{6}$$

In this equation, $u(\Gamma,\,z^*)$ is a potential energy felt by an adsorbing molecule which is at a distance z^* from the point where it first touches the surface. Since the potential is a function of the charge at the surface u is a function of the adsorbed amount. D' is an effective diffusion coefficient for the adsorption event, and kT has its usual meaning. The integral is taken over the entire path where the potential differs from the bulk value. In our approach we assume that as soon as one segment makes contact with the surface the chain is adsorbed. We neglect the resistance that the chains meets in the process of spreading out, i.e. motion towards the surface is the rate determining step in the attachment process.

At this point it is important to realize that the potential energy experienced by an entering polymer chain depends on the polymer conformation, since the chain potential energy is a sum over the potential energies of all the monomers, and these feel different energies at different distances from the wall. Chains having one monomer at distance z^* whilst other segments are positioned at distances $z > z^*$ will experience less resistance than a chain having more than one segment at z^*. We now suppose that, for each z, the polymer explores all possible configurations (with appropriate Boltzmann weighting) with one segment at $z = z^*$ and all other segments at $z > z^*$. Hence, $\exp(u(\Gamma,\,z^*)/kT)$ is actually a partition function (with respect to large distance) which therefore will be denoted as $Q_\infty/Q(z^*)$ [10], where $Q(z^*)$ and Q_∞ are partition functions of a chain with its closest monomer at $z = z^*$ (in the proximity of the surface) or at large distance from the surface (in the bulk) respectively.

Such a partition function is readily evaluated using the numerical procedure first proposed by Scheutjens and Fleer ([18], ch 4 of [4]). In this method, end-point probabilities $G(z;\ s)$ are calculated for walks on a lattice consisting of s steps and ending at z. This can be done such that the walks are restricted to the half space $z \geqslant z^*$; we denote these end-point probabilities as $G^{z^*f}(z;\ s)$. The walks are generated taking into account the interactions of segments with their surroundings, i.e. they take place in the 'field' which represents these interactions. Obviously, $z^* = 1$ corresponds to tails belonging to an adsorbed chain; we therefore restrict the calculation to $z^* > 1$. If two such walks, one of length s, and one of length $N - s + 1$, are connected at z^*, one obtains a polymer chain with a length of N segments which is just at a distance z^* from the touching point. The associated probability is $G^{z^*f}(z;\ s)G^{z^*f}(z;\ N - s + 1)$. Summing this probability over all values of s from unity to N (and correcting by a factor G^{z^*} for the double counting of segment s which occurs in both walks), we obtain the required partition function $Q(z^*)$:

$$Q(z^*) = 1/G^{z^*} \sum_{s=1}^{N} G^{z^*f}(z;\ s)G^{z^*f}(z;\ N - s + 1). \tag{7}$$

An similar expression for Q_∞ can be obtained. In the lattice model $\exp(u(z^*)/kT)$ is not a continuous function but it has discrete values in each lattice layer. Thus $R_b(\Gamma)$ is expressed in the lattice model as

$$R_b(\Gamma) = \int \frac{1}{D'} \frac{Q_\infty}{Q(z^*)}\, \mathrm{d}(z^*/l) \cong \frac{1}{D'} \sum_{z^*=2}^{z_\infty} \frac{Q_\infty}{Q(z^*)} \tag{8}$$

where z_∞ defines the layer where $Q_\infty/Q(z^*) = 1$. Furthermore it is assumed that D' does not depend on the position of the moving chain. The model employed to generate $u(z^*)$ profiles was the multi-Stern-layer approach first discussed by Böhmer *et al* [19]. The polyelectrolyte solution, containing as basic units (charged) polymer segments, solvent molecules, and free ions, fills a lattice, such that each lattice cell contains exactly one unit. Short-range (contact) interactions, such as those occurring between various units, or between units and the substrate, are taken into account by means of Flory–Huggins type interaction parameters. Electrostatic energies are incorporated by including an electrostatic Boltzmann term in the probability for each charged species (polymer segments and salt ions [19]), and calculating the electrostatic potential by a discrete version of the Poisson equation. All densities and potentials are averaged in planes of lattice sites parallel to the surface (mean-field approximation); correlations in the parallel directions are ignored. As discussed in [19], this is an acceptable description for sufficiently high polymer densities (where lateral interaction between the chains becomes important) and monovalent ions in aqueous solution. The equilibrium density profile along z (the normal to the adsorbent plane) for each of the components is calculated in a self-consistent manner, using the field to generate the conformations, and deriving a density profile, and hence a field from the weighted sum over all conformations. In this way, equilibrium polyelectrolyte density profiles, and their associated adsorbed amount Γ, can be calculated for any imposed equilibrium concentration, so that the adsorption isotherm is known. Using the density profiles, the barrier height can be immediately calculated as prescribed by equation (8).

It should be no surprise that the resistance is largely of electrostatic origin. Indeed, the resistance R_b calculated by the method described above is for neutral molecules almost negligibly small when compared to realistic values of R_t. Hence, we are dealing with an electrostatic double-layer repulsion between two particles of like charge. Because we have assumed a homogeneous density parallel to the surface, the repulsive interaction energy u_{el} (per unit area) calculated is that for two charged flat plates approaching each other.

According to standard double-layer theory [12], u_{el} can be expressed in the minimum dimensionless potential y_m between the two plates in a 1–1 electrolyte solution:

$$u_{el} = -2c_{salt}kT \int_{\infty}^{z^*} \left(\cosh\left(y_m(z^*)\right) - 1\right) \mathrm{d}z^* \tag{9}$$

where c_{salt} is the particle concentration of a 1–1 electrolyte.

3. Results

3.1. Choice of parameters

SCF calculations were performed for a cubic lattice with a spacing $l = 0.5$ nm. All interaction parameters, except the interaction between polymer segments and the surface (χ_s) were chosen to be zero. Relative permittivities ε_r were set to 80 for all components. Calculations were performed for polymers with a chain length of 100 segments, and the total number of lattice layers in the system was also set equal to 100. Our numerical calculations are restricted to $\chi_s = 5$; in the analytical model we used various values of χ_s.

Numerical integrations of equation (5) were obtained by use of a stepsize-adapted fourth-order Runge–Kutta algorithm [20]. In each step the solution is calculated for two intervals with stepsize h and one interval using stepsize $2h$. If the relative difference between the solutions is less than 10^{-5}, the stepsize is doubled. The value of R_t^{-1} was taken to be 10^{-6} m s^{-1}, in accordance with typical experiments in an impinging jet flow cell. The diffusion coefficient D' was chosen as 10^{-12} m^2 s^{-1}, which is a typical value for a polymer of about 100 segments.

In the following, the adsorbed amount will be represented in terms of the surface coverage in monolayers θ, i.e. the number of segments in adsorbed chains per lattice site. For comparison with experiment, θ can be readily converted into Γ (p 472 of [4]). The salt concentration is given as a volume fraction (ϕ_{salt}). The conversion of ϕ_{salt} to c_{salt} depends on lattice spacing and Avogadro's number [21]; for a cubic lattice with $l = 0.5$ nm one obtains $c_{salt} = 13\phi_{salt}$ (c_{salt} in mol l^{-1}).

3.2. Adsorption equilibrium

Before paying attention to the kinetics of adsorption, we first consider adsorption at equilibrium (θ_{eq}). In our discussion we will restrict ourselves to adsorption of strong (quenched) polyelectrolytes. A possible approach is to use the numerical self-consistent-field model as proposed by Böhmer *et al* [19]. However, for our discussion of trends it is just as instructive to use the analytical approximation proposed by Fleer [22]. Fleer considers the adsorption of polyelectrolytes on a *neutral* surface under the action of a non-electrostatic ('specific') interaction, the strength of which is given by the parameter χ_s. The crucial assumption of the theory is that the polymer chains adsorb in flat conformations, i.e., all segments are in contact with the wall, and the contribution of loops and tails to the adsorbed amount is negligible. Comparisons with numerical calculations using the full Böhmer theory have shown that this assumption is justified for cases where the electrostatic interactions are dominant, i.e. where the polyelectrolytes are strongly charged and the salt concentration is not extremely high [22]. In order to preserve electroneutrality, the charge of the adsorbed segments, which is given by the product of the segment charge z_p and the amount of adsorbed segments θ_{sp}, must be compensated by a diffuse layer of countercharge. According to the Gouy–Chapman theory, the total charge in such a layer is proportional to

$\varepsilon_r\kappa \sinh(y/2)$, where κ is the inverse Debye length, and ε_r the relative dielectric constant. Since we are dealing with lattice calculations, we rewrite this as $0.67\sqrt{\phi_{salt}}\sinh(y/2)$, where y is the dimensionless potential of the adsorbed layer at the surface, normalized with respect to kT, and the proportionality constant of 0.67 [22] takes the properties of the lattice and the dielectric properties of water at room temperature into account.

The adsorbed amount θ_{sp} can be expressed in terms of y and the non-electrostatic affinity χ_s for the surface: $\theta_{sp} = 1 - \frac{3}{2}\exp(z_p y - \chi_s)$. Hence, θ_{sp} must be solved from the following implicit expression:

$$z_p\theta_{sp} = z_p\left(1 - \tfrac{3}{2}\,\mathrm{e}^{z_p y - \chi_s}\right) = 0.67\sqrt{\phi_{salt}}\sinh(y/2). \tag{10}$$

For $z_p > 0.5$ the surface potential y attains a value of about four. For such high values $\sinh(y/2)$ may be approximated as $\frac{1}{2}\exp(y/2)$. In the special case where $z_p = 1$ the surface potential can be immediately calculated from a quadratic equation in $\exp(y/2)$, yielding

$$\mathrm{e}^{y/2} = \tfrac{1}{3}\,\mathrm{e}^{\chi_s}\left(-\tfrac{1}{3}\sqrt{\phi_{salt}} + \sqrt{\tfrac{1}{9}\phi_{salt} + 6\,\mathrm{e}^{-\chi_s}}\right) \tag{11}$$

which gives, in combination with equation (10), an explicit expression for the adsorption as a function of the salt concentration.

Assuming that the total adsorption at a *charged* surface can be written as the sum of a charge compensation contribution ($\theta_{cc} = -z_s/z_p$) and a specific contribution θ_{sp} as described above, the total adsorption, as a function of surface charge and salt concentration, can be readily obtained from the analytical model. In figure 1 the adsorbed amount at $\phi_{salt} = 10^{-3}$ is shown as a function of the segment charge for four values of χ_s. For comparison, the adsorbed amount calculated with the lattice model at $\chi_s = 5$ is also given (dashed curve). All curves show a decrease in the adsorbed amount as the segment charge increases. Because χ_s determines the potential and, hence, the charge at the surface, a higher affinity for the surface will allow more charges in the surface layer, resulting in a higher adsorption. As can be seen from the curves for $\chi_s = 5$ the results obtained with the one-layer model agree reasonably with the full numerical calculations based on the Böhmer theory. In figure 2 we show the adsorption of a polyelectrolyte ($z_p = 1$) as a function of the surface charge density (z_s) at various salt concentrations. It is not our purpose to discuss the discrepancies between the two models but merely to illustrate that general trends can easily be obtained with the analytical model. In our discussion on the kinetics we will use the data calculated with the original Böhmer model.

3.3. Kinetics

As pointed out in the previous section, charged polymer chains approaching the surface will feel a repulsion that increases as the surface charge due to adsorbed polymers builds up. In figure 3, the ratio $Q_\infty/Q(z^*)$ is shown as a function of the distance from the surface for a neutral surface covered with polyelectrolyte up to a coverage of 0.1 and for five volume fractions of 1–1 electrolyte. Of course, at large distance from the surface the incoming chain does not feel the presence of charged segments at the surface, $Q(z^*) = Q_\infty$. As the polymer approaches the surface the presence of adsorbed segments hampers the motion towards the surface. As can be seen, the resistance increases strongly with the distance to the surface (note the logarithmic scale), in particular if the salt concentration is low.

At relatively large separation, the potential in the region where the double layers of surface and incoming polymer overlap are low, so a Debye–Hückel approximation makes sense. Hence, we can write in the overlap region for the electrical potential of the surface layer $\sim\exp(-\kappa z)$ and for the approaching polymer $\sim\exp(-\kappa(z^* - z))$. The dimensionless

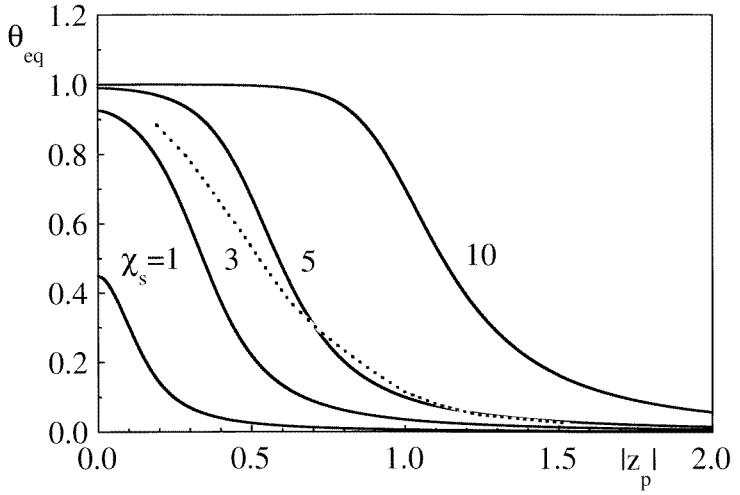

Figure 1. Adsorbed amount as a function of the segment charge for four values of χ_s and $\phi_{salt} = 10^{-3}$. The dashed curve shows the adsorption calculated with the Böhmer SCF lattice model for a chain with $r = 100$.

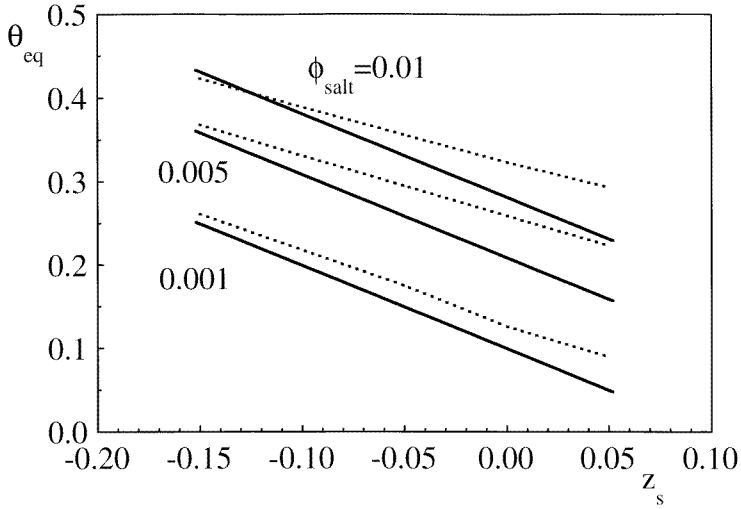

Figure 2. Adsorption at equilibrium of a strong polyelectrolyte ($z_p = 1$) as a function of the surface charge for three volume fractions of 1–1 electrolyte. Solid curves are calculated with the analytical model, dashed curves with the Böhmer SCF model.

electric potential in the overlap region (y_t) can reasonably be approximated by the sum of the two individual potentials [23]. The distance where the minimum in y_t (y_m) is situated is easily obtained from minimizing y_t with respect to z. Realizing that for small y_m $\cosh(y_m)$ can be approximated as $1 + y_m^2/2$ one can easily show from equation (8) that u_{el} is proportional to $(\phi_{salt}/\kappa)\ \exp(-\kappa z^*)$. When the logarithm of u_{el}/kT is plotted against z^*, a straight line is indeed observed for small double-layer overlap (figure 4).

The shape of the potential profiles as given in figure 3 shows a resemblance to

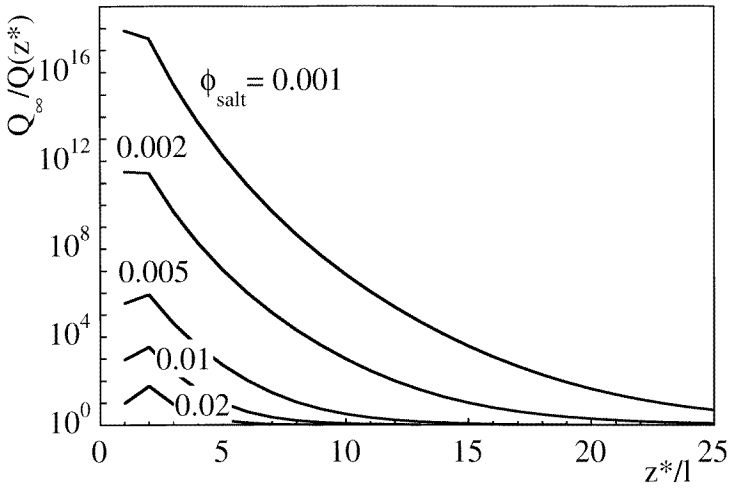

Figure 3. Resistance for polyelectrolyte ($z_p = -1$) approaching an equally charged surface. The bare surface is uncharged. Curves are calculated for $\theta_{eq} = 0.10$ for five volume fractions of 1–1 electrolyte.

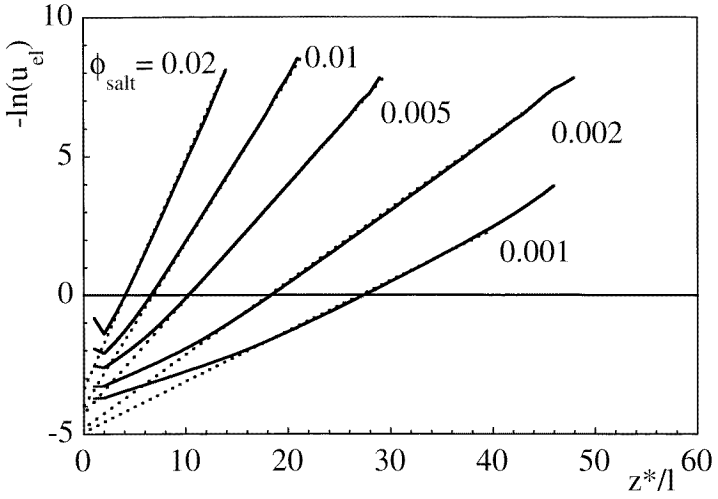

Figure 4. Logarithm of repulsive potential as a function of the separation distance z^* between polyelectrolyte and surface. The meaning of the dotted lines is explained in the text.

the interaction curve of colloidal particles. In fact, the processes of coagulation and polyelectrolyte adsorption are quite comparable. The classical Fuchs theory [24] for the rate of slow coagulation considers diffusion of a particle in a force field produced by the other particle. The force field has a repulsive part which comes from the overlap of the double layers of the coagulating particles. In addition, there is an attractive part arising from the Van der Waals interaction between the particles. In a similar way, there is a short-range attraction between the polyelectrolyte and the surface which shows up as a break in the resistance curve at $z^* = 1$. When the profiles given in figure 3 are plotted semi-logarithmically (as done in figure 4) straight parallel lines are found, which shows

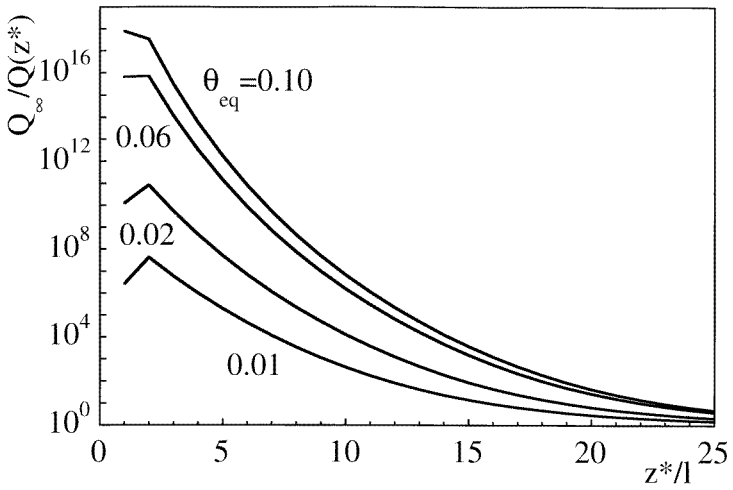

Figure 5. Resistance for a polyelectrolyte ($z_p = -1$) approaching a polymer-covered surface for $\phi_{salt} = 10^{-3}$. The bare surface is uncharged; curves are calculated for several values of θ_{eq} (i.e. for different stages in the adsorption process).

once more that we are dealing with double-layer overlap of two flat plates. The effect of increasing adsorption on the resistance is illustrated in figure 5. As more charges accumulate at the surface, diffusion towards the surface will become less likely.

As pointed out above the curves in figures 3 and 5 can be considered as resistances that a polyelectrolyte meets on its way to the surface. By adding the resistances in all layers, the barrier for adsorption is obtained (equation (6)). In figure 6 R_b is given as a function of the adsorbed amount, i.e. in different stages of the adsorption process, for five volume fractions of 1–1 electrolyte. As anticipated, R_b is an increasing function of θ_{eq}.

In the SCF model $Q(z^*)$ is calculated by means of a walk on a lattice. The weight of a step in a layer is a function of the volume fraction of the components in that layer, i.e. the potential in the Boltzmann factor depends on volume fractions introducing the self-consistency in the lattice model (ch 4 of [4]). As a lattice layer becomes more occupied with a component, the probability of making a step towards that layer decreases. When a layer is completely filled with a component stepping towards that layer is not allowed. Applied to the surface layer this means that motion of a polymer towards the surface layer is not allowed as the surface layer is completely filled with polymer segments (i.e. at saturation of the surface). The manner in which R_b is calculated takes saturation of the surface layer automatically into account, i.e. R_b will diverge to infinity as the volume fraction of segments at the surface approaches unity.

At high salt concentrations a gradual increase in the barrier is observed. Due to the large screening, repulsion only manifests itself at short distances from the surface. Decreasing the salt concentration increases the adsorption barrier dramatically. At low surface coverage there is a moderate barrier for adsorption; as more segments adsorb, the barrier increases very steeply (note the logarithmic scale for R_b). Again, we note the similarity with coagulation kinetics. The effectiveness of collision (W) leading to coagulation is determined by the potential barrier of the process. It turns out that W is almost entirely determined by the value of the potential at the maximum of the interaction curve of the coagulating particles, i.e. the contributions at short distances dominate the barrier resistance. A similar observation can be

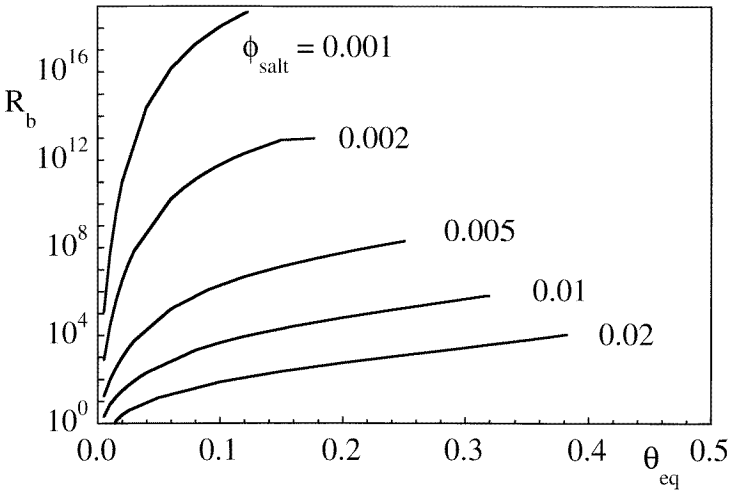

Figure 6. Potential barrier R_b for the adsorption of a polyelectrolyte ($z_p = -1$, $r = 100$) on an uncharged surface in different stages of the adsorption process. Volume fractions of 1–1 electrolyte are indicated in the figure.

made from figures 3 and 6. Particularly for low salt concentrations the main contributions to R_b originate from layers close to the surface.

Once the barrier for the adsorption is known one can calculate the adsorption as a function of time. In figure 7 the adsorption on an uncharged surface as a function of time is calculated for five volume fractions of salt. At low surface coverages the adsorption increases linearly in time. This is the regime where mass transport from the bulk solution towards the surface is the rate determining step in the adsorption process. In this stage the adsorption is not determined by salt concentration since the adsorption barrier is too small to have any effect on the adsorption rate. As more segments become attached to the surface, the barrier for adsorption increases. When the barrier exceeds the resistance R_t for the transport process the increase in adsorption is no longer linear in time. Now the attachment step determines the adsorption rate. On relatively short timescales, a levelling off in the adsorption is observed for all salt concentrations, as if saturation had been obtained. However, this is not true for all curves. In the case of $\phi_{salt} = 0.02$ the adsorption corresponding to equilibrium is indeed reached. The curves for $\phi_{salt} = 0.002$ and lower reach pseudo-plateau levels which do not correspond to equilibrium. This is seen more clearly from figure 7(b) where the adsorption is plotted against the time on a logarithmic scale. The end-points of the curves correspond to the adsorption at equilibrium for a polymer concentration of 300 mg l^{-1} (volume fraction 10^{-4}). As the figure clearly illustrates, the time needed to reach equilibrium depends strongly on the salt concentration. In the case of moderate salt concentration ($\phi_{salt} = 0.005$–0.02) the equilibrium in the adsorption is reached within a timescale comparable to that used in adsorption experiments (10^3–10^5 s). Adsorption equilibrium is not reached for low salt concentrations.

The features that are observed for the adsorption on an uncharged surface also show up for an oppositely charged surface ($z_s = 0.15$). Figure 8 shows R_b for a positively charged surface onto which a negative polyelectrolyte adsorbs. At $\theta_{eq} < 0.15$, the surface charge is incompletely compensated by adsorbed polyelectrolyte, so that the net charge seen by incoming segments is opposite to the charge of the segments, and there is no barrier. As

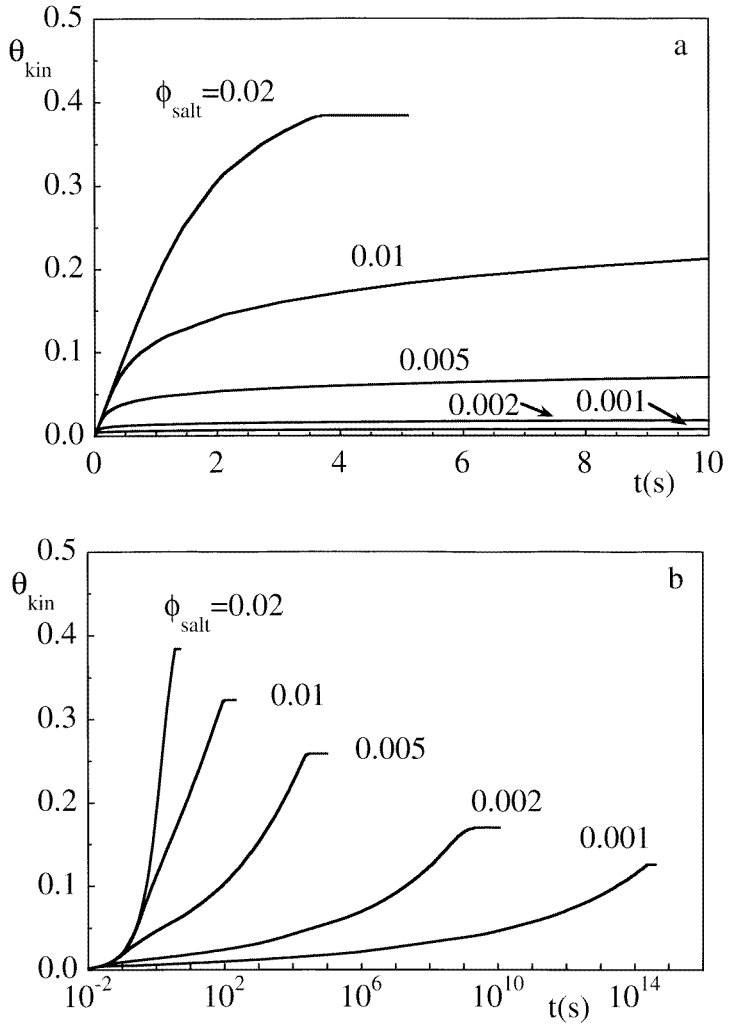

Figure 7. Adsorption of a polyelectrolyte ($z_p = -1$) on an uncharged surface as a function of time for five volume fractions of 1–1 electrolyte: (a) the adsorption on a short timescale; (b) the adsorption for long times (note the logarithmic scale). Endpoints in (b) are for equilibrium adsorption and a polymer concentration of 300 mg l^{-1} (volume fraction 10^{-4}).

soon as the surface charge is compensated, a repulsive potential is felt by the incoming chains, which shows up in an increase in the adsorption barrier. Comparing the curves in figures 6 and 8 it appears that the curves for the charged surface at $\theta_{eq} = 0.15$ nearly coincide with those for θ_{eq} at the uncharged surface, indicating that the net charge at the surface is an important parameter that determines the potential barrier.

The calculated time-dependent adsorption on the oppositely charged surface is given in figure 9. The region where mass transport determines the adsorption rate is almost entirely restricted to $\theta_{eq} < 0.15$ (surface charge is not yet compensated by polyelectrolyte). As soon as the surface charge is compensated the adsorption reaches a pseudo-plateau for low salt concentrations. Equilibrium is reached for moderate salt concentrations ($\phi_{salt} = 0.005$–0.02), but not for low salt concentrations. The abrupt ending of the time-dependent

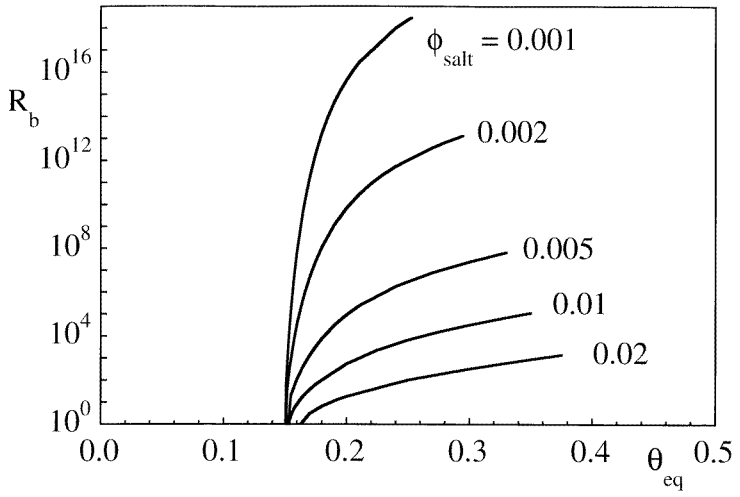

Figure 8. Potential barrier R_b for the adsorption of a polyelectrolyte ($z_p = -1$, $r = 100$) on an oppositely charged surface as a function of surface coverage θ_{eq}. Salt concentrations (1–1 electrolyte) are indicated in the figure.

adsorption curves stems from the shape of the adsorption isotherm. The calculated isotherms (not shown in this paper), i.e. θ_{eq} as a function of the equilibrium concentration, are of the high-affinity type. At (very) low concentrations the adsorption increases steeply. The adsorbed amounts corresponding to the end-points in the time-dependent adsorption curves are nearly reached for low concentrations ($\sim$0.3 mg l^{-1}). The high-affinity character of the isotherm implies that $c_{eq} - c_b$ in equation (5) is only equal to zero when θ_{kin} approaches θ_{eq} very closely. Since c_{eq} approaches c_b so abruptly the adsorption also ends abruptly.

In the previous paragraphs we have mainly considered the influence of the salt concentration on the adsorption. The influence of the surface charge (z_s) is illustrated by means of figure 10. In this figure the adsorption is given as a function of z_s. The full curves represent the adsorption calculated at $t = 1000$ s. For comparison we show the corresponding adsorption at equilibrium, as calculated with the lattice model (dashed curves). For $\phi_{salt} = 0.005$ the kinetically limited adsorption is rather close ($\sim$75%) to its equilibrium value. For the two highest salt concentrations θ_{kin} coincides with the equilibrium adsorption. However, for $\phi_{salt} = 0.001$ and 0.002, θ_{kin} is much smaller than θ_{eq}, in particular if the bare surface charge becomes small. Hence figure 10 illustrates again the pronounced influence of the salt concentration on the adsorption kinetics. Comparing θ_{kin} with the amount θ_{cc} corresponding to charge compensation, it turns out that θ_{kin} is simply the sum of θ_{cc} and an non-electrostatical contribution, which for $z_s \geqslant 0$ does not depend on the surface charge. This is because R_b depends on the *net charge* of the surface layer (figures 6 and 8). The large divergence between kinetically limited adsorption and equilibrium adsorption with decreasing surface charge can now easily be understood. The relative contribution of θ_{cc} increases as the surface charge increases. Eventually, charge compensation will have the main contribution to the adsorption and θ_{kin} will approach θ_{eq}. At decreasing surface charge θ_{cc} also decreases so the influence of the barrier on the total adsorbed amount becomes more important, thereby increasing the difference between θ_{kin} and θ_{eq}.

In figure 11 the ratio between the adsorption after 1000 s and the adsorption at equilibrium is given as a function of the polymer charge. For a polyelectrolyte with a small

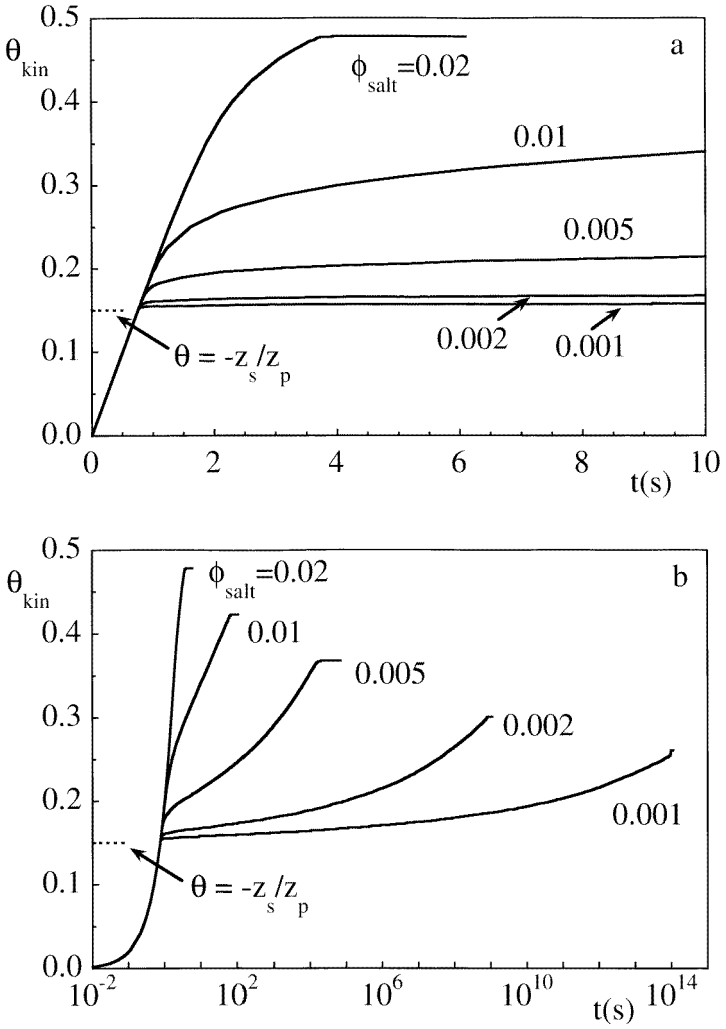

Figure 9. Adsorption of a polyelectrolyte ($z_p = -1$) on a charged surface ($z_s = 0.15$) as a function of time for five volume fractions of 1–1 electrolyte. The point where surface charge is compensated by the adsorbed polyelectrolyte is indicated. (a) The adsorption on a short timescale; (b) the adsorption for long times (note the logarithmic scale). End-points in (b) are for equilibrium adsorption and a polymer concentration of 300 mg l^{-1} (volume fraction 10^{-4}).

z_p, the adsorption approaches that of an uncharged polymer. Since effects of electrostatics are small, the adsorption is not hampered by an electrostatic barrier, hence the ratio θ_{kin}/θ_{eq} approaches unity. As the segment charge increases the adsorption will be increasingly affected by an electrostatic barrier, thereby increasing the difference between θ_{kin} and θ_{eq}. Upon increasing the segment charge, both θ_{kin} and θ_{eq} will decrease, however not to the same extent. Initially the former decreases more strongly; at large z_p the decrease in θ_{eq} dominates. Consequently, beyond about $z_p = 0.7$ the ratio θ_{kin}/θ_{eq} increases again. For high segment charge it is obvious that only small adsorptions, even at equilibrium, are possible.

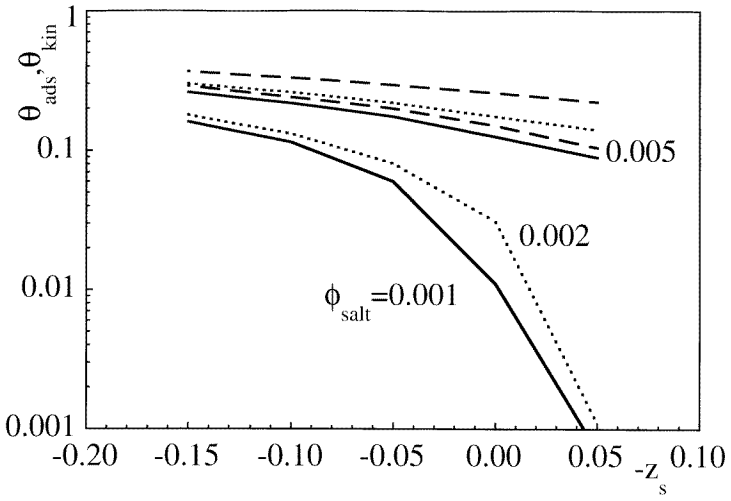

Figure 10. Influence of surface charge z_s on polyelectrolyte adsorption ($z_p = -1$) at three salt concentrations (indicated). The full curves represent the adsorption calculated at $t = 1000$ s (θ_{kin}); dashed curves represent the equilibrium adsorption calculated with the lattice model (θ_{eq}).

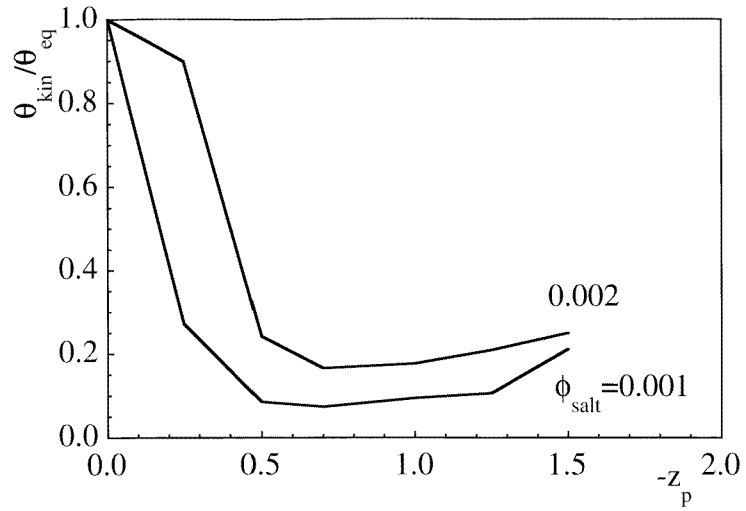

Figure 11. Influence of the segment charge z_p on the kinetically limited adsorption θ_{kin}, as determined at $t = 1000$ s.

4. Discussion

Our results show very convincingly the large effect that an electrostatic barrier has upon the rate of adsorption. Qualitatively, most of the results could be anticipated using arguments from the DLVO theory for the stability of lyophobic colloids which treats the interaction between two rigid charged particles. The present theory deals explicitly with flexible chain molecules with many internal degrees of freedom. From the results it seems that this does not change the interaction in a qualitative way. To what extent the molecular flexibility has

a quantitative influence remains to be studied.

In our model, the attractive part of the polymer–surface interaction has a very short range. As a consequence, the adsorption kinetics depends exclusively on the electrostatic part of the interaction. The equilibrium adsorbed mass, however, is strongly influenced by χ_s. As a result, the discrepancy between the equilibrium and the kinetically limited adsorption becomes larger as χ_s increases. This implies that reversibility is most likely to be found for systems where χ_s is small or even zero; this seems to be supported by experiments [25].

All our calculations have been performed for the case of a polyelectrolyte and a surface with a fixed charge density (quenched system). In the literature equilibrium adsorption for annealed systems (with a pH-dependent charge) has also been considered [22, 26]. In terms of DLVO interactions, the former case can be compared to the case of constant charge, whereas the latter case corresponds to a constant potential. It is well known that the constant-potential case leads to weaker repulsion at short distances, but that coagulation rates are qualitatively very similar for both cases. We therefore expect that the present calculations are also relevant for the adsorption kinetics of annealed polyelectrolytes.

In our approach we have used a mean-field model, i.e. discrete charges are smeared out in a layer. In real systems, charges are often localized so that discrepancies of our model with experiments can be expected. The localization of charges will manifest itself mostly at low adsorption where the surface coverage is rather heterogeneous. At large distance from the surface the smearing out of charges is a reasonable approximation. As a polymer approaches a surface more closely the electric field generated by adsorbed molecules becomes inhomogeneous. If a chain approaches locally a surface with bare spots it can pass more easily through the barriers raised by adsorbed chains. Hence, the barrier for adsorption is expected to be less than when the charges are smeared out; at low ϕ_{salt} our model tends to overestimate the adsorption barrier, i.e. the adsorption is underestimated. As the surface coverage increases the approximation of smearing out of charges is more plausible; the adsorption is less underestimated for higher ϕ_{salt}. On the other hand our model tends to overestimate the adsorption since the process of spreading is not taken into account.

We finally comment on the experiments with carboxy methyl cellulose (CMC) presented in [15]. Clearly, these data show a large difference in adsorbed amounts between a case where the pH is kept fixed during adsorption and a case where a pH cycle (high/low/high) is applied. It is therefore tempting to conclude that the adsorption at fixed pH is kinetically blocked, and that the cycle leads to an adsorbed amount closer to equilibrium. However, this is at variance with the observation that even at an ionic strength as high as 0.5 M there is still a substantial effect of cycling the pH. According to our calculations, the barrier resistance should be negligible under such conditions so that equilibrium is reached. Evidently the CMC/oxide system has features not covered by the present treatment.

In our opinion the discrepancies between our model and experiment can be attributed to an incomplete description of the desorption step. It is beyond the scope of this paper to discuss the desorption step in detail: we limit ourselves to a brief remark. It is likely that the localized interactions, e.g. ion pairs between polyelectrolyte and charged surface sites or the formation of strong (chemical) bonds [27], play an important role in the desorption process. Due to the interaction with the surface, a barrier will be present for the desorption, which is high in the case of ion pairs or strong chemical bonds. As soon as surface bonds are broken desorption becomes possible. Flexible chains can desorb their segments one by one. Experimentally, this may show up as an increase of the (hydrodynamic) layer thickness of the adsorbed layer. Complete desorption will take place if the number of segments in

contact with the surface is below some critical value. The critical number decreases as the interaction with the surface becomes stronger. Desorption of semi-flexible or rigid chains will occur less gradually as compared to flexible chains. The rigidity of the chain does not permit a desorption of segments one by one. Each desorption step involves a number of segments roughly given by the persistence length. The barrier for the desorption of rigid chains will therefore be higher than for flexible chains.

5. Conclusions

Adsorption of polyelectrolytes at low ionic strength on surfaces providing a short-range, non-electrostatic attraction is kinetically blocked by an adsorption barrier of electrostatic origin. The height of this barrier, and its effect on the adsorption kinetics, was generally calculated by combining the argument based on the Kramers theory of reaction rates with the Scheutjens–Fleer–Böhmer self-consistent-field theory for polyelectrolyte chains near a charged interface. The theory explains why the adsorbed amounts found in experiments always correspond closely to charge neutralization, as if specific interactions with the substrate do not exist, and why hysteresis should be expected upon cycling the pH, i.e., the polymer charge density.

Acknowledgment

The authors want to thank Dr F A M Leermakers for valuable discussions while preparing this paper. This work was carried out with financial support of the Dutch National Innovation Oriented Programme Carbohydrates (IOP-k).

References

[1] Kraus G and Dugone J 1955 *Ind. Eng. Chem.* **47** 1809
[2] Grant W H, Smith L E and Stromberg R R 1975 *Faraday Discuss. Chem. Soc.* **59** 209
[3] Cohen Stuart M A, Fleer G J and Scheutjens J M H M 1984 *J. Colloid Interface Sci.* **97** 526
[4] Fleer G J, Cohen Stuart M A, Scheutjens J M H M, Cosgrove T and Vincent B 1993 *Polymers at Interfaces* (London: Chapman and Hall)
[5] Frantz P, Leonhardt D C and Granick S 1991 *Macromolecules* **24** 1868
[6] Johnson H E, Douglas J F and Granick S 1993 *Phys. Rev. Lett.* **70** 3267
[7] Dijt J C, Cohen Stuart M A and Fleer G J 1994 *Macromolecules* **27** 3219
[8] Dijt J C, Cohen Stuart M A and Fleer G J 1994 *Macromolecules* **27** 3229
[9] Dijt J C, Cohen Stuart M A and Fleer G J 1992 *Macromolecules* **25** 5416
[10] Semenov A N and Joanny J F 1995 *J. Physique* II **5** 859
[11] Kramers H A 1940 *Physica* **7** 284
[12] Verweij E J W and Overbeek J Th G 1948 *Theory of Stability of Lyophobic Colloids* (Amsterdam: Elsevier)
[13] Meadows J, Williams P A, Garvey M J, Harrop R A and Phillips G O 1988 *Colloids Surf.* **32** 275
[14] Luckham P F and Klein J 1984 *J. Chem. Soc. Faraday Trans.* I **80** 865
[15] Hoogendam C W, de Keizer A, Cohen Stuart M A and Bijsterbosch B H 1997 *Proc. 7th Conf. on Colloid Chemistry (Eger, 1996) Langmuir* to be submitted
[16] Cohen Stuart M A and Fleer G J 1996 *Annu. Rev. Mater. Sci.* **26** 463
[17] Dabros T and van de Ven Th G M 1983 *Colloid Polym. Sci.* **261** 694
[18] Scheutjens J M H M and Fleer G J 1979 *J. Phys. Chem.* **83** 1619
Scheutjens J M H M and Fleer G J 1980 *J. Phys. Chem.* **84** 178
[19] Böhmer M R, Evers O A and Scheutjens J M H M 1990 *Macromolecules* **23** 2288
[20] Press W H, Teukolsky S A, Vetterling W T and Flannery B P 1992 *Numerical Recipes* (New York: Cambridge University Press)
[21] Israels R 1994 Adsorption of charged diblock copolymers *Thesis* Wageningen Agricultural University p 58

[22] Fleer G J 1996 *Ber. Bunsenges. Phys. Chem.* **100** 936
[23] Hunter R J 1987 *Foundations of Colloid Science* vol 1 (Oxford: Clarendon)
[24] Fuchs N 1934 *Z. Phys.* **89** 736
[25] Hoogeveen N G, Cohen Stuart M A and Fleer G J 1996 *J. Colloid Interface Sci.* **182** 146
[26] Borukhov I, Andelman D and Orland H 1995 *Europhys. Lett.* **32** 499
[27] Liu Q I and Laskowski J S 1989 *J. Colloid Interface Sci.* **130** 101